

UNCLASSIFIED

Defense Technical Information Center  
Compilation Part Notice

ADP013666

TITLE: Direct Numerical Simulation of Supersonic Turbulent Ramp and Step Flow

DISTRIBUTION: Approved for public release, distribution unlimited

This paper is part of the following report:

TITLE: DNS/LES Progress and Challenges. Proceedings of the Third AFOSR International Conference on DNS/LES

To order the complete compilation report, use: ADA412801

The component part is provided here to allow users access to individually authored sections of proceedings, annals, symposia, etc. However, the component should be considered within the context of the overall compilation report and not as a stand-alone technical report.

The following component part numbers comprise the compilation report:

ADP013620 thru ADP013707

UNCLASSIFIED

# DIRECT NUMERICAL SIMULATION OF SUPERSONIC TURBULENT RAMP AND STEP FLOW

I. KLUTCHNIKOV AND J. BALLMANN

*Mechanics Department*

*RWTH Aachen, University of Technology*

*D-52062 Aachen, Germany*

## Abstract

Direct numerical simulations of compressible fluid flow are performed for subsonic and supersonic channel flow with two symmetrically backward facing steps and for a supersonic compression ramp flow field. Spatial derivatives are represented by a central scheme of high order difference operators ( $N=2,4,6,8,\dots$ ) that is used together with artificial dissipation of order  $N$ . A two-step Richtmyer scheme is employed for time integration. In regions with steep gradients flux-corrected transport (FCT) according to Boris and Book is applied. Preliminary results are presented for Mach number 1.5 in case of the channel flow and further results for Mach number 2.84 in case of the ramp with a ramp angle of 24 degrees.

## 1. Introduction

The Reynolds Averaged Navier-Stokes equations (RANS) are often used in connection with various turbulence models to model technical problems of compressible fluid flow, e.g. [1]. But the aptitude of a particular turbulence model for the problem to solve is generally not known beforehand and may even be unsatisfactory. On the other hand, the rapidly growing computer resources offer a promising future to physically more realistic mathematical models like Large-Eddy Simulation (LES) and Direct Numerical Simulation (DNS), see for example [2][3]. Both methods require high order discretization with special treatment of shocks or steep gradients. While LES still needs some modeling to account for the spatially underresolved stresses, DNS should be apt to resolve all turbulent scales without the support of any empirical turbulence modeling. While the method in [3] employs alternating upwinding using compact differences, the method applied in this

paper is based on central high order numerical operators for interpolation and approximation in space in conjunction with a two-step Richtmyer scheme. The method represents an extension of the concept proposed in [4] for the Burgers' equation and the Euler equations to the system of the Navier-Stokes equations for heat conducting compressible fluid flow [5]. Flux-Corrected Transport (FCT) according to Boris and Book has been implemented to account for steep gradients, e.g. in the presence of shocks.

## 2. Numerical Method

### 2.1. INTERIOR POINTS OF THE SOLUTION DOMAIN

Denoting by  $U$  the set of conserved variables  $\rho, \rho u, \rho v, \rho w, \rho e_{total}$  and by  $F^c$  the fluxes corresponding to the inviscid and by  $F^d$  the dissipative part of the fluxes and leaving out body forces and body energy supply the system of Navier-Stokes equations reads

$$U_t + \sum_{r=1}^3 F_r^c = \sum_{r=1}^3 F_r^d \quad (1)$$

The equations are integrated with respect to time employing a second order Richtmyer scheme. Space discretization is performed with central high order numerical operators [4][5]. The numerical scheme requires artificial dissipation of the highest order of the scheme for numerical stability in the sense of von Neumann [5]. Using lower index  $i_r$  for discretization in the space directions  $r, r = 1, 2, 3$  and upper index  $n$  for time stepping the set of discretized equations reads

$$\begin{aligned} U_{i_r+1/2}^{n+1/2} &= L_r U_{i_r+1/2}^n - 0.5 \lambda_r A_{ri_r+1/2}^n R_r U_{i_r+1/2}^n \\ U_{\bullet}^{n+1} &= U_{\bullet}^n - \sum_{r=1}^3 \lambda_r \{ (F_{ri_r+1/2}^{cn+1/2} - F_{ri_r-1/2}^{cn+1/2}) \\ &\quad + (F_{ri_r+1/2}^{dn} - F_{ri_r-1/2}^{dn}) - (S_r U_{i_r+1/2}^n - S_r U_{i_r-1/2}^n) \} \\ i_r &= \{i, j, k\} \quad , \quad \Delta t / \Delta x_r =: \lambda_r \quad , \quad r = 1, 2, 3 \end{aligned} \quad (2)$$

Therein  $L_r, R_r, S_r$  represent the aforementioned high order operators,  $L_r$  serving for interpolation,  $R_r$  for approximation and  $S_r$  for artificial dissipation.  $A_r$  is the Jacobian. With coefficients  $a_m$  in  $L_r$ ,  $b_m$  in  $R_r$ , and  $d_m$  in  $S_r$  the operators of order  $N$  are defined as follows,

$$L_r U_{i_r+1/2} = \sum_{m=1}^{N/2} (-1)^{m+1} a_m (U_{i_r+m} + U_{i_r-m+1}), \quad (3)$$

$$R_r U_{i_r+1/2} = \sum_{m=1}^{N/2} (-1)^{m+1} b_m (U_{i_r+m} - U_{i_r-m+1}), \quad (4)$$

$$S_r U_{i_r+1/2} = \alpha_{i_r+1/2} \sum_{m=1}^{N/2} (-1)^{m+1} d_m (U_{i_r+m} + U_{i_r-m+1}), \quad (5)$$

with  $\alpha_{i_r+1/2}$  a prescribed factor for each cell index. The expression for the artificial dissipation of order N is

$$-\alpha \frac{\partial^N U}{\partial x_r^N} \Delta x_r^N = -(S_r U_{i_r+1/2} - S_r U_{i_r-1/2}) \Delta x_r^{-1}, \quad (6)$$

with  $\alpha$  a number to be chosen. Optionally, in domains with steep gradients FCT is applied in a self-controlled fashion with the following expressions for the anti-diffusive flux (index ad) and the corrected flux (index cor)

$$F_{ri_r+1/2}^{c(ad)} = F_{ri_r+1/2}^{c(h)n+1/2} - F_{ri_r+1/2}^{c(l)n+1/2}, \quad F_{ri_r+1/2}^{c(cor)n+1/2} = c_{i+1/2} F_{ri_r+1/2}^{c(ad)}. \quad (7)$$

The coefficients  $a_m$ ,  $b_m$  and  $d_m$  in Eq. (3), (4), and (5) are depending on the order N which is chosen for the solution [4][5].

## 2.2. BOUNDARY POINTS

At solid walls the no slip condition is prescribed and walls are assumed thermally adiabatical. The central scheme of order N makes use of N/2 fictitious points by mirror principle. For solution points at artificial boundaries marking the boundary of the computational domain, e.g. at inflow and outflow, also N/2 fictitious points are needed. Different conditions are to be distinguished in the fictitious points there for subsonic and supersonic flow. For subsonic inflow and outflow part of the values in the fictitious points are set using Riemann invariants according to a concept of local simple waves in the sense of gasdynamics while the other part of the values are extrapolated. This way non-physical reflections from the artificial boundary are mostly suppressed.

## 2.3. APPLICATION PROCEDURE AND VALIDATION

The examples we discuss in this paper would represent two-dimensional flow fields in case of laminar flow. The calculation starts as for laminar flow. On the inflow boundary at a wall a starting boundary layer with parabolic velocity profile is prescribed which may become later on changed as part of the solution because of locally subsonic inflow. At walls the correct boundary conditions are introduced from the first iteration step.

First, some thousands of time steps of the solution are performed for two-dimensional flow. Then during a certain number of time steps a disturbance consisting of two additional velocity components in the cross-plane of the main flow direction is superposed to the boundary condition at the entrance of the solution domain which makes the flow three-dimensional. Thereafter this disturbance is removed.

Numerous and extended validation tests which are not presented in the paper have been conducted for the method [5][11], e.g. comparison was made with analytical solutions of the Burgers' equation, of the 1D Riemann problem for the Euler equations, and of the mean velocity distributions in the viscous layer and the logarithmic layer from turbulent boundary layer theory. Results for compressible flow at Mach number  $M=0.2$  in a straight channel at Reynolds number  $Re=1750$  have been compared with DNS results [6][7] and experimental results at comparable Reynolds numbers [8][9]. Numerical results for a Mach 0.2 flow with  $Re=2600$  through a channel with a backward facing step were compared with experimentally determined values [10] including the Reynolds stresses at different positions behind the step [5][11]. A kind of self-validation is the check of asymptotic convergence with increasing the order  $N$  first and then refining the grid. This has been done e.g. in [11] for the flow through a channel with a straight axis and a symmetric jump of the channel height from  $h$  on the upstream side to  $3h$  on the downstream side. Data for Mach and Reynolds numbers were  $M=0.6$  and  $Re=10^4$ . Asymptotic convergence was found for  $N=8$ .

### 3. Simulations of Supersonic Flow Fields

A Mach 1.5 flow through the aforementioned channel with two symmetrical backwards facing steps has been simulated. Static pressure in the flow just before and just behind the steps has the same value  $p=1$ . The Reynolds number based on the step height  $h$  is  $Re=10^4$ . The length of the solution domain from the steps to the outflow end is  $16h$ . Number of grid cells in this domain is  $256 \times 61 \times 41$ . Flow is from left to right. Computation is started with given supersonic inflow upstream of the steps including a boundary layer of thickness  $0.15h$  at the upper and lower wall with a parabolic velocity profile. In Fig.(1) results of the density distribution are shown for orders from  $N=2$  up to  $N=16$  for the same physical time  $t=20$  which means 20000 time steps. The flow field is not yet fully established. Comparing the contour lines for the different orders one recognizes that contrary to the subsonic  $M=0.6$  case the order  $N=8$  seems not sufficient for asymptotic convergence. Before the order step from  $N=14$  to 16 the solution exhibits decreasing but still remarkable changes with increasing order. The long time simulation was then conducted with order 16. In Fig.(2) some results obtained so far

are presented. The instantaneous contour lines of Mach number, pressure and density distributions for  $t=70$  show on the inflow side the typical jet behavior for the case of adapted pressure. Then the jet becomes declining more and more, exhibiting vortical structures, local supersonic pockets at vortices and shocklets. The ranges of Mach number are from  $M=0.1$  to  $M=2.8$  and of pressure and density from  $p=0.3$  to  $p=2.3$  and  $\rho=0.4$  to  $1.7$ , respectively. Pressure fluctuations for the time interval from  $t=40$  to  $t=100$  have been recorded in points  $P_1: x_1 = 3h, x_1 = 2h, x_3 = 0$  and  $P_2: x_1 = 15h, x_2 = 2h, x_3 = 0$ . The graphs and frequency spectra do not yet represent fully developed turbulent flow. It seems that the computational domain is not long enough to observe the full transition region. Further investigations are necessary. As a second example the supersonic flow over a  $24^\circ$  ramp is revisited [11] Mach number and Reynolds number are  $M=2.84$  and  $Re=10^7$ . According to experiments by Settles [12][13], results are depicted in Fig.(3). The length of the separation zone is reproduced fairly well by the simulation, and the three-dimensional character of the flow is obvious. The pressure signature in the middle of the corner line is within a range of  $p=1.9$  to  $p=3.3$ . The mean pressure is overpredicted in the separation zone but fits fairly well the experimental values outside. The skin friction coefficient fits best the earlier experimental values found by Settles [12]. That agrees with recent results [2].

## References

1. Rodi W., Mansour N.N. (1993) Low Reynolds number k-e modeling with the aid of direct simulation data, *J. Fluid Mech.* 250, pp. 509-529
2. Rizzetta, D.P. and Visbal, M.R. (2001) Large-Eddy Simulation of Supersonic Compression-Ramp Flows, *AIAA paper 2001-2858*
3. Fezer A., Kloker M. (1998) Transition Processes in Mach 6.8 Boundary Layers at Varying Temperature Conditions Investigated by Spatial Direct Numerical Simulation, *Notes on Numerical Fluid Mechanics*, Vol. no. 72, pp. 138-145
4. Zalesak S.T. (1984) A Physical Interpretation of the Richtmyer Two-Step Lax-Wendroff Scheme, and its Generalization to Higher Spatial Order", *Adv. In Comp. Meth. For Part. Diff. Eq.*, Publ. IMACS, pp. 491-496
5. Klutchnikov, I. (1998) *Direct numerical simulation of turbulent compressible fluid flow*. Habilitation thesis (in Russian), Russian Academy of Sciences, Moscow
6. Kim J., Moin P., Moser R.D. (1987) Turbulence Statistics in Fully Developed Channel Flow at Low Reynolds Number, *J. of Fluid Mech.* 177, pp. 133-166
7. Spalart P.R. (1988) Direct simulation of a turbulent boundary layer up to  $R=1410$ , *J. of Fluid Mech.* 187, pp. 61-98
8. Whan G.A., Rothfus R.R. (1959) *Amer. Inst. Chem. Eng. J.*, Vol. no. 5, N2, pp. 205-208
9. Patel V.C., Head M.R. (1969) Some Observations on Skin Friction and Velocity Profiles in Fully Developed Pipe and Channel Flows, *J. Fluid Mech.*, Vol. no. 38, N1, pp. 181-201
10. Komarov P.L., Polyakov A.F. (1996) *Investigation About the Characteristics of Turbulence and Heat Exchange in a Channel Behind a Backward Facing Step*. Preprint IVTAN N2-396, Moscow, 70p. (in Russian)

11. Klutchnikov I., Ballmann J. (2001) DNS of Turbulent Compressible Fluid Flow with a High Order Difference Method, AIAA paper 2001-2542
12. Settles G.S., Vas I.E., Bogdonoff S.M. (1976) Details of a Shock-Separated Turbulent Boundary Layer at a Compression Corner, *AIAA Journal*, Vol. 14, No. 12, pp. 1709-1715
13. Settles G.S., Dodson L.J. (1991) Hypersonic Shock/Boundary-Layer Interaction Database, AIAA paper 1991-1763

#### 4. Figures

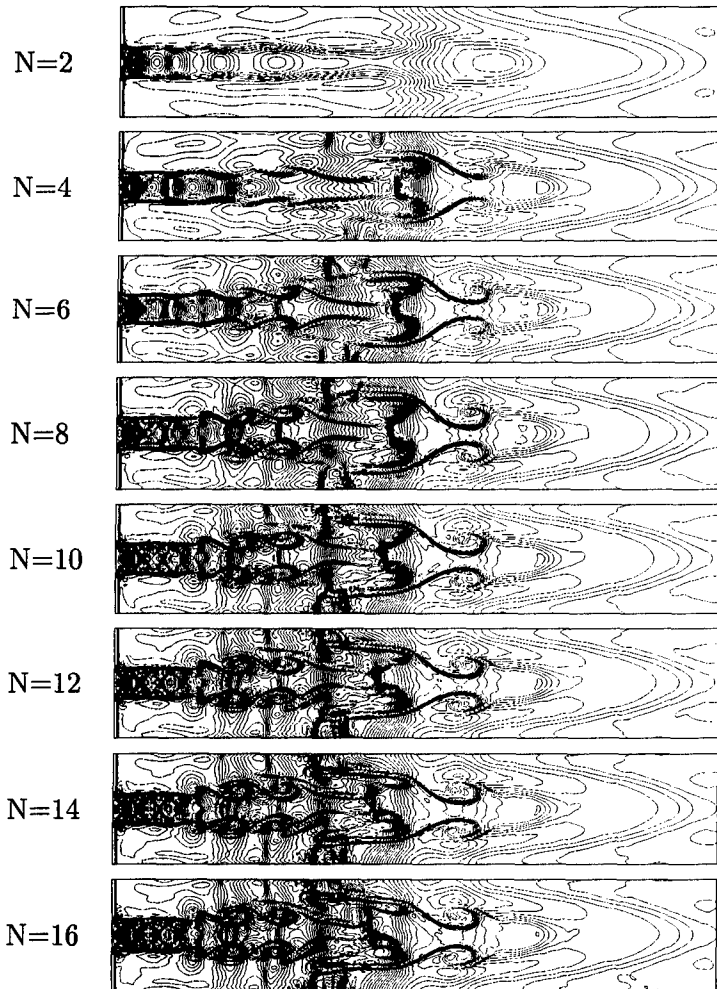


Figure 1. Supersonic flow ( $M=1.5$ ,  $Re=10^4$ ) through a channel with two backwards facing steps. Asymptotic convergence check of the instantaneous density field with increasing order,  $t=20$

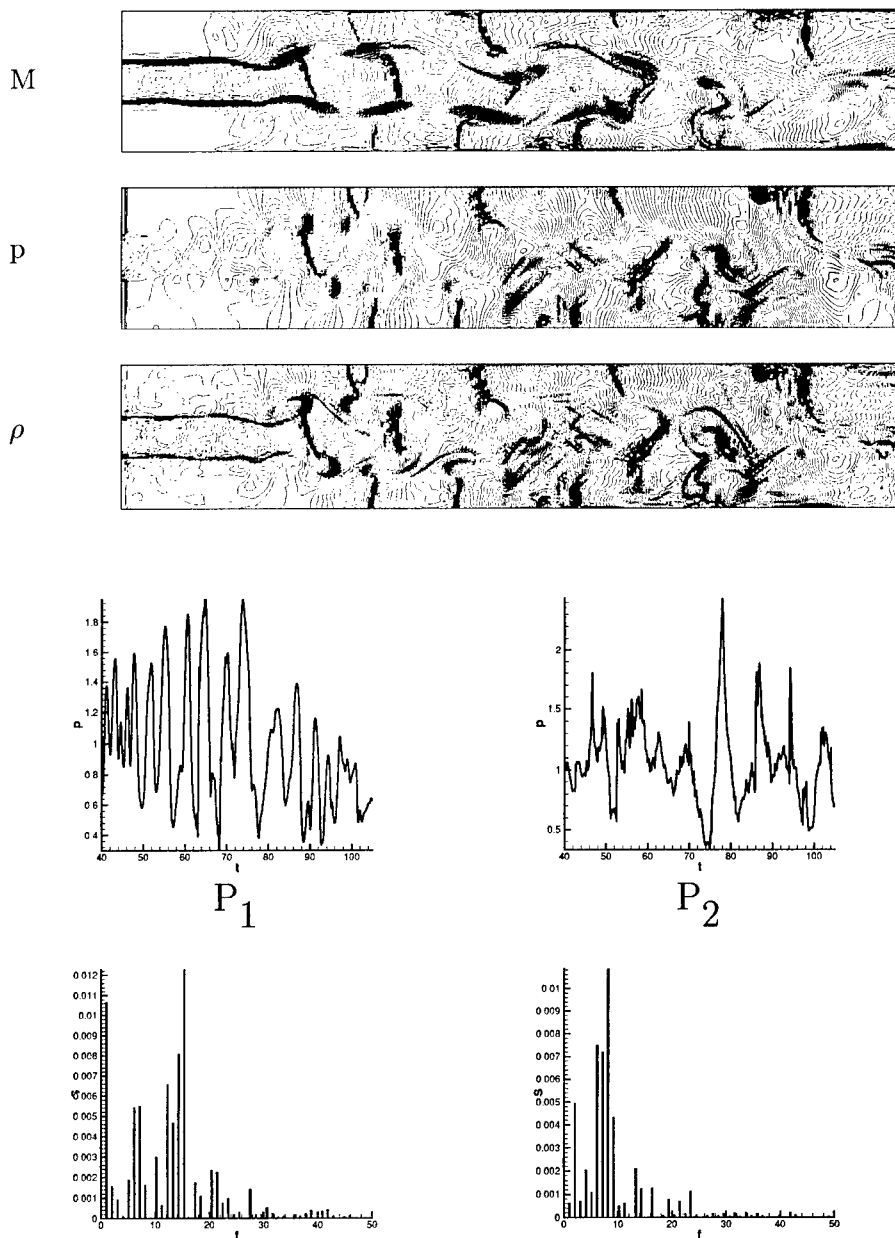


Figure 2. Supersonic channel flow ( $M=1.5$ ,  $Re=10^4$ ), instantaneous contours of Mach number, pressure and density for time  $t=70$  and signatures of pressure over time from  $t=40$  to  $t=100$  in points  $P_1$ :  $x_1 = 3h$ ,  $x_2 = 2h$ ,  $x_3 = 0$  and  $P_2$ :  $x_1 = 15h$ ,  $x_2 = 2h$ ,  $x_3 = 0$ . Lower figures: respective Fourier spectra



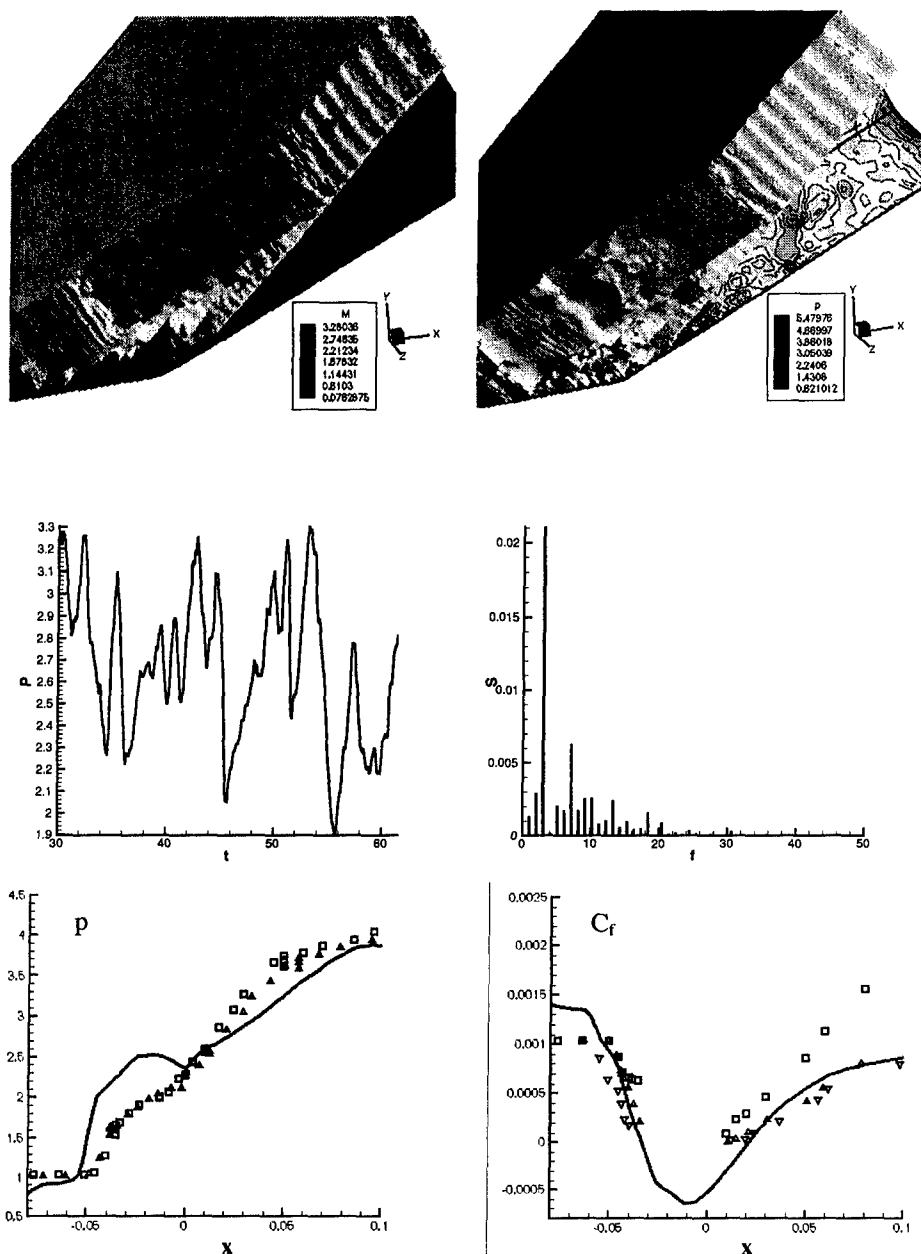


Figure 3. Supersonic flow along a  $24^\circ$  compression ramp ( $M=2.84$ ,  $Re=10^7$ ), isosurfaces of  $M=2.74$ ,  $2.5$  and  $2.05$  and  $p=2.58$  and  $1.54$  (upper figures), graph of pressure signature in the middle point of the corner line for the time interval from  $t=30$  to  $t=60$  and the respective Fourier spectrum (middle figures) and mean wall distributions of pressure  $p$  and skin friction coefficient  $c_f$  (lower figures). Symbols represent experimental values [12][13]